

# Realization of fiber-based laser Doppler vibrometer with serrodyne frequency shifting

Yanlu Li,\* Stijn Meersman, and Roel Baets

Photonics Research Group (Department of Information Technology), Ghent University-Interuniversitair Micro-Elektronica Centrum, Sint-Pietersnieuwstraat 41, 9000 Gent, Belgium

\*Corresponding author: Yanlu.Li@intec.ugent.be

Received 4 January 2011; revised 9 April 2011; accepted 11 April 2011;  
posted 14 April 2011 (Doc. ID 140343); published 9 June 2011

We demonstrate a laser Doppler vibrometer (LDV) based on the serrodyne frequency shifting technique. A proof-of-principle system is implemented on the basis of fiber-optic components but opens the way toward an ultracompact integrated LDV system on a silicon chip. With a low laser power of  $50\ \mu\text{W}$ , the serrodyne LDV was able to measure submicrometer vibrations with frequencies in the audio range. © 2011 Optical Society of America

*OCIS codes:* 130.3060, 130.3120, 120.5060, 120.5050.

## 1. Introduction

Laser Doppler vibrometers (LDVs) have been exploited in a wide variety of applications, such as acoustics [1], aerospace [2], and hearing research [3]. They allow the measurement of the instantaneous time-dependent velocity of a vibrating surface by measuring the Doppler shift induced on the laser frequency. However, the flexibility of commercialized LDVs is still limited by the size of the equipment. For many applications, such as multichannel vibrometry, miniaturization can be of great value [4,5]. Miniaturized LDVs could also have other advantages over bulk and fiber-based LDVs, such as low power consumption and low fabrication cost. Our proposal for a miniaturized LDV is based on silicon photonics, a complementary metal oxide semiconductor (CMOS)-compatible technology platform allowing the integration of different microphotonic devices (e.g., waveguides, couplers, lasers, and modulators) and making low-cost mass production possible [6–10]. With this technology, an LDV can be fabricated on an ultracompact silicon-on-insulator (SOI) chip with an area smaller than  $1\ \text{mm}^2$ .

Many methods have been developed for modulation and demodulation schemes in LDV systems, such as two-frequency interferometry [11] and synthetic-heterodyne demodulation [12]. The most classical method for bulk LDV devices is the heterodyne detection method because of its good sensitivity and high reliability [13–15]. In recent years coherent detection has seen a very important revival in the field of telecommunication due to the introduction of high-speed analog-to-digital conversion of the heterodyne signal and subsequent digital signal processing, but this approach requires a lot of power-hungry digital electronic processing [16].

Optical frequency shifters (OFSs) are typically required in the heterodyne system. Bragg cells, which can realize a frequency shift by using the acousto-optic effect, are the most commonly used OFSs in free-space heterodyne LDVs. However, it is very challenging to realize acousto-optic Bragg cells on SOI. The main reason relates to the difficulty of generating acoustic waves on the patterned SOI chips. We propose the use of the serrodyne technique on the basis of phase modulators for generating frequency shifts [17,18]. Compared with sinusoidal phase shifting techniques [19], serrodyne frequency shifting (SFS) requires a higher bandwidth for the phase modulator. However, high-speed (higher than 10 GHz) phase modulators on SOI have been

reported recently [20,21], with enough bandwidth for the SOI-based SFS. Additionally, generating a sinusoidal phase modulation on the SOI chip is not very simple, since the optical phase change and the applied voltage in the phase modulator are nonlinearly related [22]. The advantage of using simple sinusoidal driving signals in bulk LDV setups is hence not obvious in the miniaturized versions. The demodulation methods in the sinusoidal techniques are also more complicated than those in the serrodyne techniques [23,24] and therefore consume more power.

This paper presents an architecture for miniaturized serrodyne LDV devices with a limited power budget and demonstrates the proof of principle of a fiber version of this LDV system. One application with high potential is the implanted LDV-based middle ear microphone used to help hearing impaired individuals. The power consumption of the implanted LDV is strongly restricted due to the difficulty of changing batteries. In this paper, the power of the laser is restricted to around  $50 \mu\text{W}$ . This power could be low enough for an implanted battery, but still high enough to avoid distortions arising from the noises in the electronic part behind the detector. The minimum laser power is mainly determined by the ability of receiving backscattered signals from the moving target. With respect to receiving backscattered signals, a fiber system mimics the on-chip LDV. This will be further discussed in Section 3. A fiber-based LDV system is demonstrated in this paper to show the proof of principle of the SFS and to estimate the minimal detectable audible vibrations within the aforementioned power budget.

In Section 2, the theory of SFS is briefly discussed. In Section 3, the architecture of a miniaturized on-chip LDV is proposed. A fiber-based setup used to demonstrate the principle of serrodyne LDVs is described in Section 4. The measurement results on audio frequency vibrations are discussed in Section 5. The conclusions will be in Section 6 of this paper.

## 2. Serrodyne Optical Frequency Shift (SFS)

The serrodyne LDV is based on a Mach-Zender interferometer whereby a laser beam with a frequency  $f_0$  is split by an optical coupler into the reference and measurement signals. The reference signal is purposely phase modulated in a sawtooth profile  $\varphi(t) = 2\pi[tf_{\text{OFS}} - \text{floor}(tf_{\text{OFS}})]$ , where  $f_{\text{OFS}}$  is the constant frequency shift created by the SFS, and the function  $\text{floor}(x)$  returns the largest integer no larger than  $x$ . The backscattered measurement signal, according to the Doppler theory, undergoes an instantaneous frequency shift  $f_D(t) = 2v(t)f_0/c$  because of the reflection on a moving surface whereby  $v(t)$  is the instantaneous velocity of the reflector projected on the propagation direction, and  $c$  is the speed of light in the medium. The measurement and reference signals are mixed on a photodetector, and a photocurrent is generated:

$$S_o(t) \propto E_r^2 + \alpha E_m^2 + 2E_r E_m \sqrt{\alpha} \cos[2\pi f_{\text{OFS}} t - \phi_D(t)], \quad (1)$$

where  $E_r$  is the amplitude of the reference signal's electric field,  $E_m$  is the amplitude of the measurement signal's electric field before it is sent to the vibrating surface,  $\alpha$  is the optical power loss of the measurement signal, and  $\phi_D(t)$  is the phase shift due to the movement of the target. The Doppler shift  $f_D(t)$  can be calculated from the phase shift  $\phi_D(t)$  according to Eq. (2):

$$f_D(t) = \frac{d\phi_D(t)}{dt}. \quad (2)$$

The first two terms in Eq. (1) are DC and can be filtered away with low-pass filters. The Doppler shift  $f_D(t)$  can be recovered from the third term of Eq. (1) using digital quadrature demodulation techniques.

However, due to the bandwidth limit in the phase modulator, the fall time of the sawtooth signal cannot be infinitely small [25]. Many higher-order harmonic sidebands in the photocurrent signal are thus not totally suppressed, which affects the LDV's ability to recover the vibration velocity. To suppress these useless sidebands, the fall time needs to be kept small enough, which implies that the modulator driver and the modulator need to have a much larger bandwidth than  $f_{\text{OFS}}$ . Most of these sidebands can also be suppressed later in the demodulator with filters, except the  $-1$ st-order sideband, which coincides with the first-order harmonic. When the  $-1$ st-order harmonic is not negligible, the demodulated phase change can be expressed as

$$\phi'_D(t) = \arctan \left[ \frac{\sin 2\phi_D(t)}{\cos 2\phi_D(t) + \sqrt{r}} \right] - \phi_D(t), \quad (3)$$

where  $r = P_{-1}/P_1$  is the power ratio between the  $-1$ st and first harmonic sidebands. When the ratio  $r$  is quite small, which is the case for serrodyne modulation, the phase error  $e(t) = \phi'_D(t) - \phi_D(t)$  can be approximated as

$$e(t) \approx -\sqrt{r} \sin 2\phi_D(t). \quad (4)$$

## 3. Integrated LDV Based on Silicon Photonics

A fully integrated Mach-Zender-type LDV on SOI is proposed and schematically illustrated in Fig. 1. With SOI as a platform, the passive parts of the interferometer (e.g., waveguides, splitters, and fiber couplers) can be directly fabricated in the top silicon layer by means of CMOS technology. Laser sources and photo detectors can, for example, be based on InGaAsP epitaxial layers bonded on top of the chip with benzocyclobutene (BCB) as the intermediate layer [7,8]. The frequency shifter, as is proposed, can be a carrier-injection/depletion-based phase

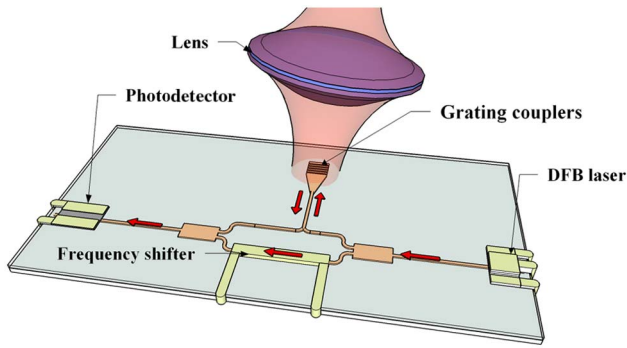


Fig. 1. (Color online) Schematic illustration of integrated LDV on SOI.

modulator [22]. As is shown by the arrows in Fig. 1, the signal from the distributed feedback (DFB) laser is split into two parts by the optical splitter. One part of the signal goes to the reference arm where the frequency shifter is placed to shift the optical frequency. The other part is sent out to the moving target from the chip through a shallow etched grating coupler [26] and a lens system that images the grating coupler on the vibrating surface. The back-scattered signal is collected back to the chip through the same grating coupler. Both reference and measurement signals are finally recombined in the optical combiner and sent to the photodetector. Since the size of the grating coupler is similar to that of a single-mode fiber core, the fiber-based LDV system discussed in Section 4 gives a good estimate of the power budget limited by the scattering loss of the reflected signals.

In a first prototype of this LDV chip, a low-speed thermo-optic (TO) phase modulator with a footprint of  $2\ \mu\text{m} \times 725\ \mu\text{m}$  was demonstrated [27]. The modulator was actually a single-mode waveguide with a Ti heater fabricated on top. The phase modulation is the result of the relatively high TO coefficient of silicon ( $1.86 \times 10^{-4}\ \text{K}^{-1}$ ). To prevent the guided mode from being absorbed by the Ti heater, a 600 nm thick BCB layer was placed in between the waveguide and the heater. By changing the heating power with a voltage signal, the effective refractive index of the guided mode in the underlying waveguide could be modulated. The driving voltage needs to have a repeating square-root-of-time profile so as to generate a sawtooth refractive index change in the guided mode. A frequency shift of only several kilohertz was generated with the TO serrodyne technique. The amount of the frequency shift was limited by the low speed of the TO effect in this device. According to the Carson bandwidth rule, with a 1 kHz OFS one can recover small vibrations ( $<380\ \mu\text{m/s}$ ) at a frequency lower than 500 Hz. In this situation, however, the measurement signal could also be easily influenced by environmental fluctuations. In order to measure real vibrations, high-speed modulators are needed. This is possible with today's state of the art carrier injection or carrier depletion silicon phase modulators.

A fiber LDV system with a higher OFS but a similar signal receiving system and the same laser wavelength (1550 nm) is studied in Section 4. It directly gives a reference for the integrated LDV with a higher-speed frequency shifter, and predicts the measuring ability of tiny movements within the defined power budget.

#### 4. Experimental Setup

A serrodyne LDV based on a single-mode fiber system was built, the schematic configuration of which is illustrated in Fig. 2.

The laser source was a DFB laser at 1550 nm, with a 3 dB linewidth of around 2 MHz. An isolator (not shown in the figure) was inserted behind the laser to avoid optical reflections to the laser. In our setup, the relative intensity noise (RIN) caused by the laser driver dominated over other noise sources when the optical power incident on the detector was higher than 100 nW. If this power was lower than 100 nW, the discretization noise from the 16 bit analog-to-digital converter (ADC) became dominant. The demodulated signal would thus be strongly distorted due to the large relative noise. To avoid the noise problem in this regime, the reflection of the measurement signal from the moving object back to the fiber needed to be enhanced. A focuser was used to focus the laser beam onto one small spot on the vibrating surface. A retro-reflective film was also attached on top of the moving surface, and it improved the reflected power by more than 10 dB. When, on the other hand, RIN dominates, the signal-to-noise ratio (SNR) can be written as

$$\text{SNR} \propto \frac{\sqrt{\alpha P_m P_r}}{\alpha P_m + P_r}, \quad (5)$$

where  $P_m$  and  $P_r$  are the powers of the measurement and reference signals just after the first optical splitter, respectively, and  $\alpha$  is the optical loss of the measurement signal after scattering. The highest SNR is obtained when  $\alpha P_m = P_r$ . Therefore, an asymmetric optical coupler was used to compensate the loss in the measurement arm.

A lithium niobate (LiNbO<sub>3</sub>) phase modulator was situated in the reference arm to generate the frequency shift. In the measurement arm, light went to the vibrating surface (a moving membrane of a loudspeaker) through a circulator and focuser (the numerical aperture is 0.1). However, a small

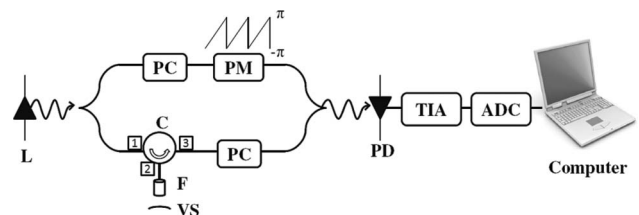


Fig. 2. Schematic configuration of the experimental setup. L, laser; C, circulator; F, focuser; VS, vibrating surface; PM, phase modulator; PC, polarization controller; PD, photodetector; TIA, transimpedance amplifier; ADC, analog-to-digital converter.

spurious fraction of light (around  $-50$  dB) went directly from port 1 to port 3 of the circulator, and the surface of focusers also introduced reflections. These signals were not exposed to the velocity information of the vibrating surface and did to some degree deteriorate the results of demodulation.

Several polarization controllers were inserted to align the polarization of the measurement and reference arms. The optical path length difference of the measurement and reference arms were set to be smaller than the coherence length of the laser so that the signals from those two arms are still coherent with each other.

In the second 3 dB optical coupler, the beams from both arms were recombined and sent to an InGaAs photodiode. The photocurrent was converted to a voltage signal by a homemade transimpedance amplifier (TIA). In the TIA, the lower-frequency signals were filtered away to reduce the influence of low-frequency noise. Then the signal was digitized with a data acquisition card (NI USB-6218). The demodulation was realized in MATLAB.

### 5. Measurement Results and Discussions

The reflected power from the moving surface was measured with an optical power meter. The optical power of the reflected signal coupled back into the fiber was measured to be 20 dB less than the power sent to the moving surface. However, it was still 30 dB above the spurious reflection from the circulator and focuser. As discussed in Section 4, in order to have a good SNR, a 99:1 optical coupler to split the light asymmetrically (99% of light was sent to the measurement arm) was used to compensate the 20 dB optical loss in the measurement arm. In our experiment, the power of the laser was reduced to  $50 \mu\text{W}$ , and the corresponding optical power on the detector was 200 nW. An SNR of 40 dB was measured.

A function generator was used to create the sawtooth phase profile. Because of the linear relation between the phase and voltage in the electro-optic effect, a sawtooth voltage was directly provided to the phase modulator. When the peak-to-peak amplitude of the sawtooth voltage was 7.08 V, a good suppression of the useless sidebands was obtained. The suppression ratio of the  $-1$ st-order mode could be estimated by the power ratio of the third- and first-order harmonics, since the spectrum of the serrrodyne OFS was rather symmetric around the first-order sideband [25]. The ratio was around  $-35$  dB, and the corresponding phase error was smaller than 5% according to Eq. (4). The limited suppression ratio was mainly caused by the imperfect polarization input to the phase modulator.

Sound vibrations at several different frequencies (between 300 and 6 kHz) produced by the membrane of a loudspeaker were then measured. The frequency shift  $f_{\text{OFS}}$  in the reference arm was set at 24 kHz. A digital bandpass filter with a center frequency of 24 kHz and a bandwidth of 12 kHz was used to filter

away the low-frequency noise and high-order harmonics.

Our measurement results were compared with those obtained from a commercial LDV instrument (Polytec OFV-5000). Both our fiber-based and Polytec LDVs were pointed to the same spot on the vibrating membrane, and the measurements were done for the same duration. Two measurement results are shown in Fig. 3. It turned out that the vibration frequencies measured by both devices matched well, while the vibration amplitudes were somewhat different (ratio  $\chi$  is 0.76). This difference may be caused by the mismatch of the measuring positions for the two devices or by inaccurate calibration.

A figure of resemblance (FOR) was defined as

$$\text{FOR} = 1 - \frac{\text{RMS}(v_P - \chi v_f)}{\text{RMS}(v_P)}, \quad (6)$$

with  $v_P$  and  $v_f$  the vibration speed measured with the Polytec LDV and our fiber LDV, respectively. The calculated FOR for different vibration frequencies  $f_{\text{vib}}(t)$  and peak velocities of the membrane of the loudspeaker are shown in Fig. 4(a).

It can be seen that the trends for all vibration frequencies were the same. At low peak velocities (around  $100 \mu\text{m/s}$ ), the FOR was rather low. This is because the phase variations in these situations were so small that they were strongly distorted by the phase noise. When the peak velocity surpassed  $300 \mu\text{m/s}$ , the FOR was higher than 60%. For peak velocity higher than  $800 \mu\text{m/s}$ , the FOR exceeded 80%. However, at even higher speeds the FOR saturated and even dropped slightly. This is because the bandwidth of our signal became larger than the bandwidth (12 kHz) around  $f_{\text{OFS}}$ . Information would then be lost after filtering, resulting in distortions. The bandwidth of the bandpass filter was increased to around  $f_{\text{OFS}}$ , and the corresponding FOR figure is shown in Fig. 4(b). The dropping part in Fig. 4(a) disappeared. But noise introduced by the larger filter

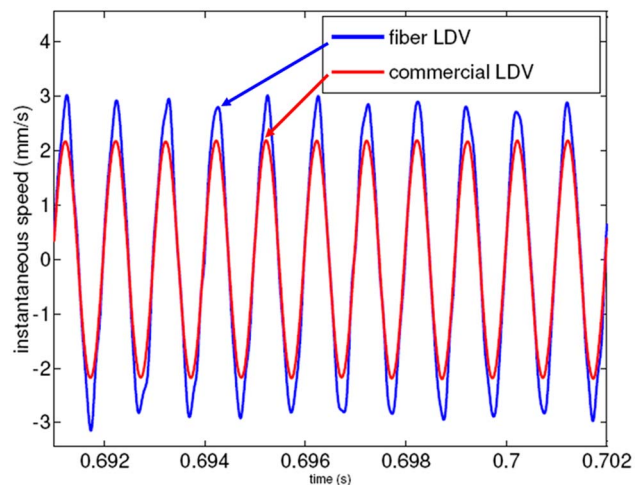


Fig. 3. (Color online) Comparison of the demodulated results between Polytec LDV and fiber-based serrrodyne LDV.

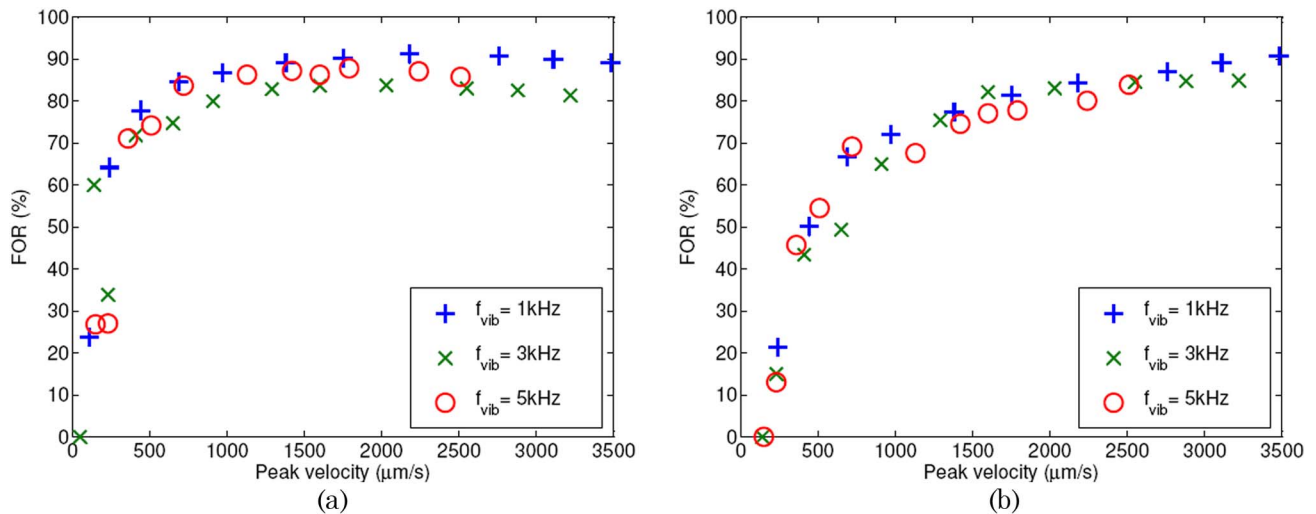


Fig. 4. (Color online) FOR for different vibration frequencies and speeds with different bandwidths of bandpass filters. (a) Bandwidth of 12 kHz. (b) Bandwidth of 24 kHz.

bandwidth deteriorated the demodulation and decreased the FOR for low-speed vibrations.

Our measured vibrations with sound frequencies starting from around  $1000 \mu\text{m/s}$  were relatively accurate, with a FOR larger than 80%. This corresponded with a peak displacement of the order of 100 nm.

## 6. Conclusions

A serrodyne frequency shifter technique was proposed and demonstrated as a candidate for the frequency shifter in a miniaturized heterodyne LDV. The theoretical analysis showed that an ideal SFS can be a perfect single sideband frequency shifter, but in practice it is limited by the bandwidth of the modulator and modulator driver. The  $-1$ st-order harmonic influenced the demodulation results and should be highly suppressed in the OFS. A fiber-based LDV system with telecommunication components (lasers and detectors) was built to make the proof of principle for on-chip LDVs working with SFS. The optical frequency shift used in the reference arm was 24 kHz. While the power of our laser (at 1550 nm) was limited to  $50 \mu\text{W}$ , our measurements on audio frequency vibrations with submicrometer displacements (larger than 100 nm) were still acceptable.

The authors acknowledge the Research Foundation—Flanders (FWO) through contract 3G003410 for partial support, as well as the Gent University—Methusalem project “Smart Photonic Chips.” They acknowledge Pieter Wiskerke, Gerald Dumm, and Patrik Kennes (Cochlear) for useful discussions about applications in hearing aids. They also thank Professor Joris Peeters, Professor Patrick Segers, Dr. Danae Delbeke, Gunay Yurtsever, and Jeroen Allaert for discussions various aspects about this work.

## References

1. P. Gren, K. Tatar, J. Granström, N.-E. Molin, and E. V. Jansson, “Laser vibrometry measurements of vibration and sound fields of a bowed violin,” *Meas. Sci. Technol.* **17**, 635–644 (2006).
2. L. Jacquin, D. Fabre, D. Sipp, V. Theofilis, and H. Vollmers, “Instability and unsteadiness of aircraft wake vortices,” *Aerospace Sci. Technol.* **7**, 577–593 (2003).
3. K. R. Whittemore, S. N. Merchant, B. B. Poon, and J. J. Rosowski, “A normative study of tympanic membrane motion in humans using a laser doppler vibrometer (LDV),” *Hear. Res.* **187**, 85–104 (2004).
4. H. van Elburg, J. Dirckx, and W. Decraemer, “High-resolution quadruple-channel heterodyne laser velocimeter based on birefringent optics,” *Optik* **119**, 497–499 (2008).
5. H. van Elburg, J. Dirckx, and W. Decraemer, “Design and performance of a high-resolution dual-channel heterodyne laser velocimeter,” *Optik* **118**, 345–349 (2007).
6. D. Vermeulen, S. Selvaraja, P. Verheyen, G. Lepage, W. Bogaerts, P. Absil, D. V. Thourhout, and G. Roelkens, “High-efficiency fiber-to-chip grating couplers realized using an advanced CMOS-compatible silicon-on-insulator platform,” *Opt. Express* **18**, 18278–18283 (2010).
7. Z. Sheng, L. Liu, J. Brouckaert, S. He, and D. V. Thourhout, “InGaAs PIN photodetectors integrated on silicon-on-insulator waveguides,” *Opt. Express* **18**, 1756–1761 (2010).
8. L. Liu, R. Kumar, K. Huybrechts, T. Spuesens, G. Roelkens, E.-J. Geluk, T. de Vries, P. Regreny, D. Van Thourhout, R. Baets, and G. Morthier, “An ultra-small, low-power, all-optical flip-flop memory on a silicon chip,” *Nat. Photon.* **4**, 182–187 (2010).
9. J. V. Campenhout, P. R. Romeo, P. Regreny, C. Seassal, D. V. Thourhout, S. Verstuyft, L. D. Cioccio, J.-M. Fedeli, C. Lagahe, and R. Baets, “Electrically pumped InP-based microdisk lasers integrated with a nanophotonic silicon-on-insulator waveguide circuit,” *Opt. Express* **15**, 6744–6749 (2007).
10. J. Brouckaert, G. Roelkens, D. Van Thourhout, and R. Baets, “Compact InAlAs–InGaAs metal–semiconductor–metal photodetectors integrated on silicon-on-insulator waveguides,” *IEEE Photon. Technol. Lett.* **19**, 1484–1486 (2007).
11. D.-C. Su, M.-H. Chiu, and C.-D. Chen, “Simple two-frequency laser,” *Precis. Eng.* **18**, 161–163 (1996).
12. Y.-L. Lo and C.-H. Chuang, “New synthetic-heterodyne demodulator for an optical fiber interferometer,” *IEEE J. Quantum Electron.* **37**, 658–663 (2001).
13. N. P. Cooper, “An improved heterodyne laser interferometer for use in studies of cochlear mechanics,” *J. Neurosci. Methods* **88**, 93–102 (1999).
14. M. Johansmann, G. Siegmund, and M. Pineda, “Targeting the limits of laser Doppler vibrometry,” in *Proceedings of the International Disk Drive Equipment and Materials Association*

- 2005 (International Disk Drive Equipment and Materials Association, 2005), pp. 1–12.
15. A. T. Waz, P. R. Kaczmarek, and K. M. Abramski, "Laser-fibre vibrometry at 1550 nm," *Meas. Sci. Technol.* **20**, 105301 (2009).
  16. G. Li, "Recent advances in coherent optical communication," *Adv. Opt. Photon.* **1**, 279–307 (2009).
  17. R. C. Cumming, "The serrodyne frequency translator," *Proc. IRE* **45**, 175–186 (1957).
  18. I. Y. Poberezhskiy, B. Bortnik, J. Chou, B. Jalali, and H. R. Fetterman, "Serrodyne frequency translation of continuous optical signals using ultrawide-band electrical sawtooth waveforms," *IEEE J. Quantum Electron.* **41**, 1533–1539 (2005).
  19. W. Jin, L. M. Zhang, D. Uttamchandani, and B. Cuishaw, "Modified J1...J4 method for linear readout of dynamic phase changes in a fiber-optic homodyne interferometer," *Appl. Opt.* **30**, 4496–4499 (1991).
  20. M. Lipson, "Compact electro-optic modulators on a silicon chip," *IEEE J. Sel. Top. Quantum Electron.* **12**, 1520–1526 (2006).
  21. W. M. Green, M. J. Rooks, L. Sekaric, and Y. A. Vlasov, "Ultra-compact, low RF power, 10 Gb/s silicon Mach–Zehnder modulator," *Opt. Express* **15**, 17106–17113 (2007).
  22. H. Yu, W. Bogaerts, and A. De Keersgieter, "Optimization of ion implantation condition for depletion-type silicon optical modulators," *IEEE J. Quantum Electron.* **46**, 1763–1768 (2010).
  23. P. de Groot, "Design of error-compensating algorithms for sinusoidal phase shifting interferometry," *Appl. Opt.* **48**, 6788–6796 (2009).
  24. K. Falaggis, D. P. Towers, and C. E. Towers, "Phase measurement through sinusoidal excitation with application to multi-wavelength interferometry," *J. Opt. A* **11**, 054008 (2009).
  25. L. M. Johnson and C. H. Cox, "Serrodyne optical frequency translation with high sideband suppression," *J. Lightwave Technol.* **6**, 109–112 (1988).
  26. G. Roelkens, D. Vermeulen, D. Van Thourhout, R. Baets, S. Brision, P. Lyan, P. Gautier, and J.-M. Fedeli, "High efficiency diffractive grating couplers for interfacing a single mode optical fiber with a nanophotonic silicon-on-insulator waveguide circuit," *Appl. Phys. Lett.* **92**, 131101 (2008).
  27. Y. Li, S. Meersman, and R. Baets, "Optical frequency shifter on SOI using thermo-optic serrodyne modulation," in *7th IEEE International Conference on Group IV Photonics, Beijing* (IEEE, 2010), pp. 75–7.